9th LISA Symposium, Paris
ASP Conference Series, Vol. 467
G. Auger, P. Binétruy and E. Plagnol, eds.

Advanced Virgo Status

J. Degallaix,[14] T. Accadia,[12] F. Acernese,[6ac] M. Agathos,[15a] A. Allocca,[8ac] P. Astone,[9a] G. Ballardin,[3] F. Barone,[6ac] M. Barsuglia,[1] A. Basti,[8ab] Th. S. Bauer,[15a] M. Bebronne,[12] M. Bejger,[17c] M.G. Beker,[15a] M. Bitossi,[8a] M. A. Bizouard,[11a] M. Blom,[15a] F. Bondu,[2b] L. Bonelli,[8ab] R. Bonnand,[14] V. Boschi,[8a] L. Bosi,[7a] B. Bouhou,[1] C. Bradaschia,[8a] M. Branchesi,[4ab] T. Briant,[13] A. Brillet,[2a] V. Brisson,[11a] T. Bulik,[17b] H. J. Bulten,[15ab] D. Buskulic,[12] C. Buy,[1] G. Cagnoli,[14] E. Calloni,[6ab] B. Canuel,[3] F. Carbognani,[3] F. Cavalier,[11a] R. Cavalieri,[3] G. Cella,[8a] E. Cesarini,[4b] E. Chassande-Mottin,[1] A. Chincarini,[5] A. Chiummo,[3] F. Cleva,[2a] E. Coccia,[10ab] P.-F. Cohadon,[13] C. N. Colacino,[8ab] A. Colla,[9ab] M. Colombini,[9b] A. Conte,[9ab] J.-P. Coulon,[2a] E. Cuoco,[3] S. D'Antonio,[10a] V. Dattilo,[3] M. Davier,[11a] R. Day,[3] R. De Rosa,[6ab] G. Debreczeni,[18] W. Del Pozzo,[15a] L. Di Fiore,[6a] A. Di Lieto,[8ab] A. Di Virgilio,[8a] A. Dietz,[12] M. Drago,[16ab] G. Endrőczi,[18] V. Fafone,[10ab] I. Ferrante,[8ab] F. Ferrini,[3] F. Fidecaro,[8ab] I. Fiori,[3] R. Flaminio,[14] L. A. Forte,[6a] J.-D. Fournier,[2a] J. Franc,[14] S. Franco,[11a] S. Frasca,[9ab] F. Frasconi,[8a] M. Galimberti,[14] L. Gammaitoni,[7ab] F. Garufi,[6ab] M. E. Gáspár,[18] G. Gemme,[5] E. Genin,[3] A. Gennai,[8a] A. Giazotto,[8a] R. Gouaty,[12] M. Granata,[14] G. M. Guidi,[4ab] A. Heidmann,[13] H. Heitmann,[2a] P. Hello,[11a] G. Hemming,[3] P. Jaranowski,[17d] R.J.G. Jonker,[15a] M. Kasprzack,[3,11a] I. Kowalska,[17b] A. Królak,[17ae] N. Leroy,[11a] N. Letendre,[12] T. G. F. Li,[15a] M. Lorenzini,[4a] V. Loriette,[11b] G. Losurdo,[4a] E. Majorana,[9a] I. Maksimovic,[11b] V. Malvezzi,[10a] N. Man,[2a] M. Mantovani,[8a] F. Marchesoni,[7ac] F. Marion,[12] J. Marque,[3] F. Martelli,[4ab] A. Masserot,[12] J. Meidam,[15a] C. Michel,[14] L. Milano,[6ab] Y. Minenkov,[10a] M. Mohan,[3] N. Morgado,[14] S. Mosca,[6ab] B. Mours,[12] L. Naticchioni,[9ab] I. Neri,[7ab] F. Nocera,[3] L. Palladino,[10ac] C. Palomba,[9a] F. Paoletti,[8a,3] R. Paoletti,[8ac] M. Parisi,[6ab] A. Pasqualetti,[3] R. Passaquieti,[8ab] D. Passuello,[8a] M. Pichot,[2a] F. Piergiovanni,[4ab] L. Pinard,[14] R. Poggiani,[8ab] G. A. Prodi,[16ab] M. Punturo,[7a] P. Puppo,[9a] D. S. Rabeling,[15ab] I. Rácz,[18] P. Rapagnani,[9ab] V. Re,[10ab] T. Regimbau,[2a] F. Ricci,[9ab] F. Robinet,[11a] A. Rocchi,[10a] L. Rolland,[12] R. Romano,[6ac] D. Rosińska,[17cf] P. Ruggi,[3] E. Saracco,[14] B. Sassolas,[14] D. Sentenac,[3] L. Sperandio,[10ab] R. Sturani,[4ab] B. Swinkels,[3] M. Tacca,[3] L. Taffarello,[16c] A. P. M. ter Braack,[15a] A. Toncelli,[8ab] M. Tonelli,[8ab] O. Torre,[8ac] E. Tournefier,[12] F. Travasso,[7ab] G. Vajente,[8ab] J. F. J. van den Brand,[15ab] C. Van Den Broeck,[15a] S. van der Putten,[15a] M. Vasuth,[18] M. Vavoulidis,[11a] G. Vedovato,[16c] D. Verkindt,[12] F. Vetrano,[4ab] A. Viceré,[4ab] J.-Y. Vinet,[2a] S. Vitale,[15a] H. Vocca,[7a] R. L. Ward,[1] M. Was,[11a] M. Yvert,[12] A. Zadrożny,[17e] J.-P. Zendri,[16c]

[1]*APC, AstroParticule et Cosmologie, Université Paris Diderot, CNRS/IN2P3, CEA/Irfu, Observatoire de Paris, Sorbonne Paris Cité, 10, rue Alice Domon et Léonie Duquet, 75205 Paris Cedex 13, France*

[2]*Université Nice-Sophia-Antipolis, CNRS, Observatoire de la Côte d'Azur, F-06304 Nice[a]; Institut de Physique de Rennes, CNRS, Université de Rennes 1, 35042 Rennes[b], France*

[3]*European Gravitational Observatory (EGO), I-56021 Cascina (PI), Italy*

[4]*INFN, Sezione di Firenze, I-50019 Sesto Fiorentino[a]; Università degli Studi di Urbino 'Carlo Bo', I-61029 Urbino[b], Italy*

[5]*INFN, Sezione di Genova; I-16146 Genova, Italy*

[6]*INFN, Sezione di Napoli [a]; Università di Napoli 'Federico II'[b], Complesso Universitario di Monte S.Angelo, I-80126 Napoli; Università di Salerno, Fisciano, I-84084 Salerno[c], Italy*

[7]*INFN, Sezione di Perugia[a]; Università di Perugia[b], I-06123 Perugia; Universita' di Camerino, Dipartimento di Fisica[c], I-62032 Camerino, Italy*

[8]*INFN, Sezione di Pisa[a]; Università di Pisa[b]; I-56127 Pisa; Università di Siena, I-53100 Siena[c], Italy*

[9]*INFN, Sezione di Roma[a]; Università 'La Sapienza'[b], I-00185 Roma, Italy*

[10]*INFN, Sezione di Roma Tor Vergata[a]; Università di Roma Tor Vergata, I-00133 Roma[b]; Università dell'Aquila, I-67100 L'Aquila[c], Italy*

[11]*LAL, Université Paris-Sud, IN2P3/CNRS, F-91898 Orsay[a]; ESPCI, CNRS, F-75005 Paris[b], France*

[12]*Laboratoire d'Annecy-le-Vieux de Physique des Particules (LAPP), Université de Savoie, CNRS/IN2P3, F-74941 Annecy-Le-Vieux, France*

[13]*Laboratoire Kastler Brossel, ENS, CNRS, UPMC, Université Pierre et Marie Curie, 4 Place Jussieu, F-75005 Paris, France*

[14]*Laboratoire des Matériaux Avancés (LMA), IN2P3/CNRS, F-69622 Villeurbanne, Lyon, France*

[15]*Nikhef, Science Park, Amsterdam, the Netherlands[a]; VU University Amsterdam, De Boelelaan 1081, 1081 HV Amsterdam, the Netherlands[b]*

[16]*INFN, Gruppo Collegato di Trento[a] and Università di Trento[b], I-38050 Povo, Trento, Italy; INFN, Sezione di Padova[c] and Università di Padova[d], I-35131 Padova, Italy*

[17]*IM-PAN 00-956 Warsaw[a]; Astronomical Observatory Warsaw University 00-478 Warsaw[b]; CAMK-PAN 00-716 Warsaw[c]; Białystok University 15-424 Białystok[d]; NCBJ 05-400 Świerk-Otwock[e]; Institute of Astronomy 65-265 Zielona Góra[f], Poland*

[18]*Wigner RCP, RMKI, H-1121 Budapest, Konkoly Thege Miklós út 29-33, Hungary*

Abstract.
Advanced Virgo is the successor of the initial Virgo gravitational wave detector. This new interferometer will use the infrastructure of its predecessor but aims to be 10 times more sensitive. This presentation will give an overview of the Advanced Virgo design and the technical choices behind it. The different subsystem will be detailed as well as the challenges that can be expected. Finally the up-to-date installation progress and expected schedule will be given.

1. Introduction

At the time of summer 2012, we are currently living in a period of transition for the network of laser interferometer Gravitational Wave (GW) detectors. While the first generation has been progressively decommissioned in the years 2010-2011, the second generation of interferometer will enter in operation and continue the search of GW at the corner of the years 2015-2016.

Even if no detection has been made with the initial GEO, LIGO and Virgo interferometers (respectively ref. Grote (2008); Abbott et al. (2009); Accadia et al. (2012)), important upper limits have been set on the rate and amplitude of GW events (ref. Abadie et al. (2012a,b)), putting even constraint on the physical model of the universe (ref. The LIGO Scientific Collaboration and The Virgo Collaboration (2009)).

While the first generation of interferometer was taking data, a second generation of detectors was being designed. The goal of those advanced detectors is to be 10 times more sensitive than their predecessors, increasing the volume of space probed by a factor 1000. This second generation of interferometers must guarantee the direct detection of GW on a regular basis (ref. Abadie et al. (2010)), opening a new window to study the universe.

This article is about the design and building of one of the second generation interferometers: the French-Italian Advanced Virgo interferometer. In the first part, the design of Advanced Virgo and the motivations behind it will be given. Building the interferometer and reaching the planned sensitivity will require some key technologies to be mastered. Approaches to overcome some critical challenges will be highlighted in the second part. Finally, the progression and the near future of the project will be detailed.

2. Interferometer design

In this section, the expected sensitivity of Advanced Virgo will be described and an overview of the different sub-systems will be given. The Advanced Virgo interferometer will be installed on the site of the initial Virgo detector with the new interferometer using the vacuum infrastructure of its predecessor.

2.1. Sensitivity and noise budget

The sensitivity of Advanced Virgo is presented in figure 2.1. The peak sensitivity of the interferometer is $4 \times 10^{-24}[1/\sqrt{\text{Hz}}]$ around 300 Hz.

The noises which may likely limits the sensitivity are the suspension thermal noise and the radiation pressure noise at low frequency below 50 Hz, the mirror coating thermal noise in the mid frequency range and the photon shot noise at high frequency, above 400 Hz.

From the sensitivity curve of the detector one can derive the expected inspiral ranges which indicates how far the interferometer can see a particular astrophysical source of GW optimally oriented and located in the sky. With the sensitivity curve shown in figure 2.1, the inspiral range for binary neutron stars of masses 1.5 $M_\odot$ is 134 Mpc and the inspiral range for binary black holes (30 $M_\odot$) is above one Gigaparsec, 1020 Mpc exactly.

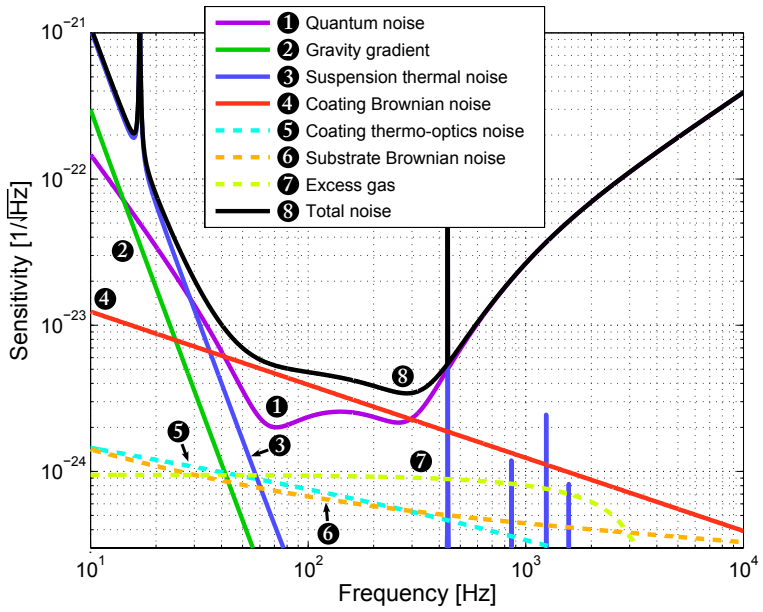

Figure 1. Expected sensitivity of the Advanced Virgo interferometer. For this plot, the signal recycling cavity has been tuned to maximise the detector sensitivity to the inspiral range for the coalescing of binary neutron stars. Prominent noise sources and their contribution to the sensitivity are also included in this plot.

2.2. Optical setup and core optics

The core of the Advanced Virgo interferometer is a dual recycling Michelson interferometer with Fabry-Perot arm cavities. The schematics of the interferometer is shown in figure 2.2.

At the final stage of Advanced Virgo, the input laser power will be 200 W, delivering 125 W at the entrance of the interferometer. The optical power inside the power recycling cavity, at the beamsplitter will be 5 kW and up to 650 kW of light will be stored in the arms. Compared to the initial Virgo, more than 100 times more light will be circulating in the arm cavities.

2.2.1. The arm cavities

The two 3 km long stable cavities are the most critical cavities regarding the quality of the optics. Those cavities are crucial to the performance of the detector, since it is where the gravitational wave signal is measured.

For the detector to reach its design sensitivity as much light as possible must be stored in the arm cavities. During the first steps of the design of Advanced Virgo a tight upper limit has been put to the acceptable amount of light loss by the cavities. The maximum amount of light loss per round trip must be less than 75 ppm. The number of 75 ppm of loss induces severe constraints on the quality of the optics and size of the laser beam. The most important consequences are reminded here:

- The mirror surface flatness (sometimes called roughness) is critical for the optical loss. Numerous optical simulations has been done to define the acceptable surface height of the low spatial frequency ($< 50\text{m}^{-1}$) defect. For Advanced Virgo mirrors it was demon-

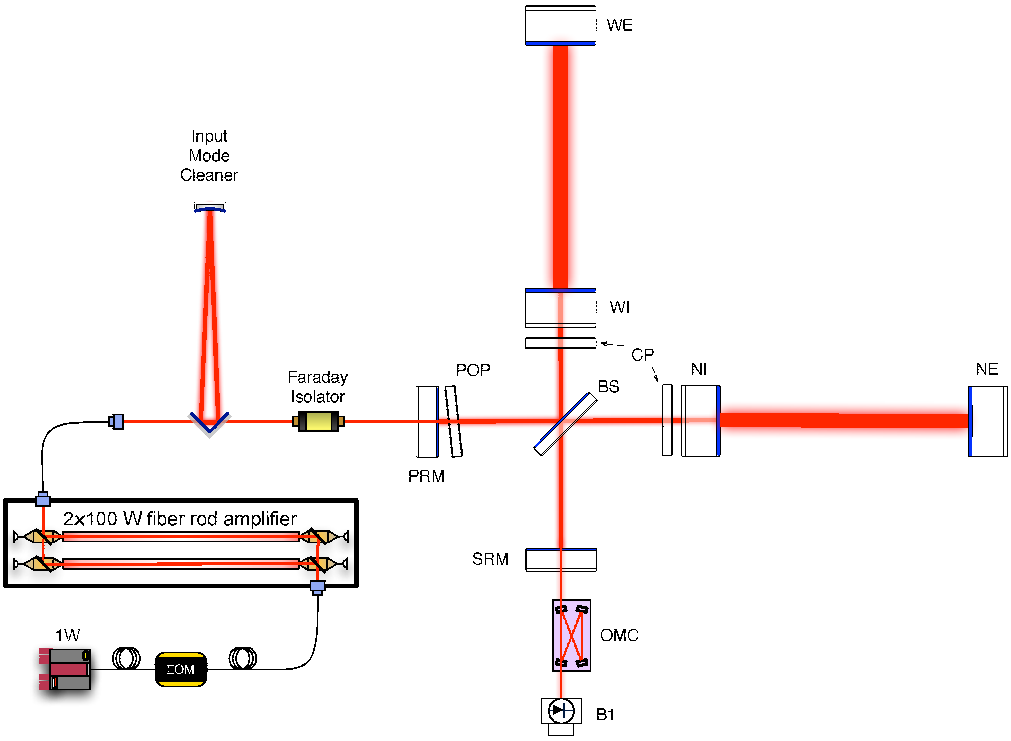

Figure 2. Layout of the Advanced Virgo detector. This illustration is not on scale since the arm cavities are 3 km long whereas the recycling cavities around the beam-splitter are 10 m long.

strated that surface height in the central diameter of 150 mm must be less than 0.5 nm RMS.

- The mirror micro-roughness scatters incident light at high angle and so can also participate to the cavity round trip losses. Based on simulations and previous experiences, the height of the micro-roughness on the central part must be less than 1 Å.
- The optical absorption of the coating must also be taken into account for the loss budget. However, the coating absorption is extremely low (less than 0.5 ppm/cm) but still high enough to create disastrous thermal effects in the interferometer.
- Since the diameter of the optics is limited to 350 mm by the manufacturer of the glass substrate, the radius of the Gaussian laser beam should be much smaller to avoid any significant amount of light falling outside the mirrors. The Gaussian beam radius on the input mirror is set to be 49 mm and 58 mm on the end mirror to give negligible clipping loss (< 1 ppm).

2.2.2. The recycling cavities

The recycling cavities are serving two goals: first the power recycling cavity is used to increase the available laser power at the beamsplitter and then the signal recycling cavity can serve to tune the sensitivity of the detector for targeted search of GW sources.

All the first generation detectors used marginally stable recycling cavities. That is to say short cavities, with no focusing element so the size of laser beam remains constant within the

cavity. Those cavities are also called degenerated since the higher order optical modes which are junk light are allowed to resonate at the same time as the fundamental TEM_{00} mode.

For the second generation of detectors, different approaches will be used. Advanced LIGO will use stable recycling cavities where the size of the laser beam is increased by a factor 9 within the input of the cavity and the arm cavities. The Advanced LIGO recycling cavities will be folded to save space and requires additional focusing and steering optics. After numerous discussions and simulations, it was chosen that Advanced Virgo will continue to use marginally stable cavities as the initial Virgo.

Even if marginally stable cavities are very sensitive to optical aberrations and require extra telescopes at the injection and detection sides, those cavities still present advantages: they are already well known since used in the first generation of detectors and are easier to control since having less optics compared to the stable cavities. Moreover, they requires less space to be built.

Even if the recycling cavities dimensions are the same between the initial and Advanced Virgo, the cavities has now some additional optics which are represented in figure 2.2. The names and roles of those optics are described below:

- The Signal Recycling Mirror (SRM) is a new mirror inserted at the dark port of the interferometer. By microscopic displacement of this mirror, one can tune the optical response of the interferometer to the GW signals.
- Two Compensation Plates (CP), one in each arm, are added in front of the arm cavity input mirror substrates. The plates are used by the thermal compensation system as actuators to reduce the aberrations in the recycling cavity.
- The Pick Off Plate (POP) in front of the power recycling mirror can sample the circulating beam in the power recycling cavities and is used to derive part of the longitudinal and angular control signals for the interferometer.

2.3. Laser and input optics

The input laser for Advanced Virgo is a 200 W fiber laser. Fiber lasers present several advantages: the design is simpler and it requires less optics compared to laser with solid state amplifiers. The laser is constituted by 2 stages: one ultra stable 1 W Nd-YAG laser is injected to two fiber amplifiers mounted in parallel. The two amplifiers are made of Ytterbium rod, able to deliver 100 W each. At the end, the beam of each amplifiers will be added coherently to deliver 200 W in total.

Before reaching the input of the interferometer, the laser beam has to pass through the injection system. This system is essential to stabilize the beam in term of frequency and amplitude and helps to decrease the beam jitter. Right at the exit of the laser, the laser beam first passes through a series of modulators which creates the sidebands fields, at four different frequencies, used to derive control signals for the interferometer.

The beam is then injected into the input mode cleaner, a 144 m long 3 mirrors cavity designed to suppress any higher order mode content from the laser beam and to reduce also the beam jitter. Finally the beam passes through a telescope where is magnified by a factor 19 to reach a beam size of 49 mm before entering the power recycling cavity.

2.4. Detection

The detection side of the interferometer is in charge of generating the error signals to keep the interferometer at its optimal working point and also to read the GW signal.

The main part of the detection system is located at the dark port of the interferometer. There, the beam exiting the interferometer from the signal recycling mirror is transmitted by the detection telescope, which is similar in design to the injection one and reduces the beam size by a factor 50. Afterward, the beam passes through two identical output mode cleaner mounted in series, to remove the sidebands and higher order modes content from the laser

beam. The output mode cleaners are four mirrors monolithic cavity made in block of fused silica of dimension 63 mm × 30 mm. Once filtered the beam is send to different single element or quadrant photodiodes for the longitudinal and angular controls of the interferometer.

Detection benches in vacuum are also inserted behind the arm cavity end mirrors and after the reflection from the pick off plate. Those benches are simplified and smaller replica of what one can find at the dark port, used again for the control of the interferometer.

2.5. Suspension

The suspensions system, based on cascaded pendulums, isolates the mirrors from the seismic motion. This system is called the superattenuator and was already present for the initial Virgo interferometer. This system only requires minor upgrades, since it is already compliant with the Advanced Virgo specifications.

However two new and compact suspension systems were designed for Advanced Virgo. The first system, in air, can isolate from the ground the optical tables supporting part of the optics for the injection and detection benches. The second system can be fitted inside a small vacuum tower and accommodates the small detection system behind the arm end mirrors. As an example, the residual motion of the bench is expected to be less than $10^{-11}\mathrm{m}/\sqrt{\mathrm{Hz}}$ at 10 Hz.

2.6. Vacuum system

The core of the vacuum system, the large 3 km long vacuum tube will be mostly left untouched by the installation of Advanced Virgo. The residual pressure in the two arms must be decreased by a factor 100 compared to the initial Virgo, reaching up to 10^{-9} mbar in the arms. This is necessary for the sensitivity of the detector to not be limited by the noise induced by the vacuum pressure (called 'excess gas' in figure 2.1).

To reach this pressure, the baking of the arm vacuum tube is necessary, however it is impossible to heat the suspension towers since the supperattenuators are already inside and can not resist to the baking temperature (150°C). So to avoid the contamination of the ultra-clean vacuum tube from the suspensions towers four cryotraps will be installed at the ends of each two arms.

2.7. Technical Design Report

If the previous sections have only opened the appetite of the reader hungry for knowledge, the detailed design of Advanced Virgo and the simulations used to validate it are available in the Advanced Virgo Technical Design Report (ref. The Virgo Collaboration (2012)).

3. Expected challenges

Reaching the design sensitivity of Advanced Virgo will not be a peaceful ride and from experiences or simulations we already know that some tasks will be difficult or risky. A selection of the some of the most expected challenges we will face are summarized in this section.

3.1. Meeting the mirror specifications

Like it was already mentioned in section 2.2.1, the flatness of the arm cavity mirrors must be below 0.5 nm RMS in the central part. To reach such a surface quality, a two steps approach must be undertaken: first, standard mechanical polishing is used to bring the substrate surface RMS around 2 nm. Then a second step must be used such as ion beam polishing where an ion beam removes all bumps at the surface of the mirrors to reduce its flatness. This technique has been used for the mirrors of Advanced LIGO.

For this second step, another technique called corrective coating has been developed in LMA. Instead of removing the bumps with an ion beam, the microscopic holes at the surface of the mirror will be filled with fused silica, the same material as the substrate. For this method, a new displacement machine has been installed in the coating chamber and the substrate is

moved in front of a thin beam of silica particles, stopping wherever material has to be added. Preliminary tests have shown that on a real size mirror, using the corrective coating, the RMS surface flatness has been decreased from 2.1 nm to 0.36 nm, so within the specification of Advanced Virgo.

3.2. The thermal compensation system

In the first generation of GW interferometers, a thermal compensation system was already present to correct the effects of the optical absorption in the coating and substrates. For Advanced Virgo, this system will be upgraded and is now a critical component, essential to achieve the required performance of the detector.

Two reasons can explain why this subsystem has gained more importance: first, the recycling cavities will be more degenerated in Advanced Virgo compared to the initial Virgo, making the cavities more sensitive to aberrations. Optical simulations have shown that even cold defects from the surface error of the mirrors or from the substrate refractive index inhomogeneity of the optics are large enough to degrade the interferometer performance. Second reason, the circulating power has been increased by a factor 16 in the recycling cavities and up to 100 for the arm cavities increasing tremendously the thermal effects.

Three main diagnostic tools will be used to measure the wavefront distortions inside the interferometer (ref. Rocchi et al. (2012)). First, phase cameras at the dark port will measure the spatial shape of the sidebands field circulating in the recycling cavities, and will estimate the distortions in the recycling cavities. Second, Hartman wavefront sensors also probing the recycling cavities will measure the change in distortions as the optical power is increased inside the interferometer. Finally, a probe beam will monitor the deformations of the high reflectivity surface of the arm cavity mirrors.

All the diagnostic tools mentioned above will derive error signals for thermal actuators in order to keep the interferometer aberration free. There main actuators with different dynamic ranges are planned. Heating rings around the main mirrors of the recycling and arms cavities can tune the radii of curvature of the mirrors. On the compensation plates, two CO_2 laser beams will be projected. One with an annular profile to correct the substrate aberration of the arm cavities input mirrors and a second beam of lower power will be scanning the plate surfaces to compensate for any non circular symmetry distortions remaining.

3.3. Managing the scattered light

The first generation of the interferometer has highlighted the susceptibility of the detector to scattered light. Some picoWatt of light scattered recombining to the main interferometer beam can be enough to spoil the detector sensitivity (ref. Hild (2007)).

The problem of scattered light will be even greater for the second generation detectors because of the larger amount of circulating light. At full power 125 W of light will be injected inside the interferometer. From all this light, roughly 20 W will be reflected back, few Watts will be absorbed and transmitted at the dark port. That means that, around 100 W of light is scattered outside the interferometer and so must be properly dumped.

Most of the scattered light happens in the arm cavity, where light could be scattered at small angle due to the mirror imperfect flatness (the 50 ppm of arm cavity round trip loss previously mentioned in 2.2.1). To avoid the scattered light to recombine in the interferometer, absorbing baffles were already inserted along the 3 km vacuum tube. For Advanced Virgo, baffles will also be installed around all the mirrors. Extensive research is now going on, to know best position, size and material for the baffles.

3.4. Suspending the optics

The way the mirror is attached to the last stage of the superattenuator is very critical since a bad design can easily increase the suspension thermal noise. Whereas in the initial Virgo, only a mirror was attached to each superattenuator with glass fibers, for Advanced Virgo the system

will be more complex. For example, for the arm cavity input playloads, not only the mirror must be attached but also a large baffle, a compensation plate and a heating ring. So a complete redesign of the last suspension stage has been done.

The new suspension system for the beamsplitter, using steel wire to suspend the optic, will be tested during the summer 2012. At the same time, a dedicated test facility with a large vacuum chamber has been setup in Roma to test the CP last suspension stage and at the end of the year the input mirror suspension. These tests will also help to check the suspension and mirror bulk quality factor before installation on site.

4. Current status

The decommissioning of the Virgo+ equipment to be replaced has started in fall 2011. To quote some of the work done: the laser lab has been emptied and the new suspended bench has been tested. Previous Virgo+ test masses has been detached from the suspension without any damage and stored. Vacuum pipe has been cut to make room for the cryotraps and wall has been pushed to prepare new clean rooms in the central building.

In parallel to the infrastructure work, procurement and building of subsystem for Advanced Virgo is the main focus of the collaboration. A non exhaustive list of advancement is given here. All the large size mirror substrates has been delivered and the call for tender for polishing will be launched during the autumn 2012. A prototype 100 W fiber laser has already been successfully tested delivering more than 90% of the its output power in the TEM_{00}. The suspended benches has been assembled and are currently tested and tuned.

5. Conclusion and timeline

At the time of writing, during the summer 2012, the Advanced Virgo project is going at full speed. While on the Virgo site, the decommissioning of the previous interferometer is almost completed and the important infrastructure work has started, the procurement and prototyping of the different subsystem is moving fast in the different laboratories of the collaboration.

The main mirrors of Advanced Virgo are expected to be coated and characterized around mid 2014 for an installation on site at the end of 2014. The commissioning of the new interferometer will start in 2015 and will last around 6 months with first a configuration similar to Virgo+ (25 W of input power and no signal recycling). The goal is to have an interferometer ready to participate to the first science run in coincidence with the Advanced LIGO interferometers.

The signal recycling mirror will be installed after 2017 and only then the input power will be raised gradually to 200 W to allow the detector to reach its maximal sensitivity.

References

Abadie, J., et al. (The LIGO Scientific Collaboration and The Virgo Collaboration) 2010, Classical and Quantum Gravity, 27, 173001

— 2012a, Phys. Rev. D, 85, 022001

— 2012b, Phys. Rev. D, 85, 102004

Abbott, B. P., et al. (The LIGO Scientific Collaboration and The Virgo Collaboration) 2009, Reports on Progress in Physics, 72, 076901

Accadia, T., et al. (The Virgo Collaboration) 2012, Journal of Instrumentation, 7, P03012

Grote, H. (The LIGO Scientific Collaboration) 2008, Classical and Quantum Gravity, 25, 114043

Hild, S. 2007, Ph.D. thesis, GEO 600

Rocchi, A., Coccia, E., Fafone, V., Malvezzi, V., Minenkov, Y., & Sperandio, L. 2012, Journal of Physics: Conference Series, 363, 012016

The LIGO Scientific Collaboration and The Virgo Collaboration 2009, Nature, 460, 7258, 990
The Virgo Collaboration 2012, Advanced Virgo Technical Design Report, https://tds.ego-gw.it/itf/tds/file.php?callFile=VIR-0128A-12.pdf